



**Precise Measurement of the  $W$  Boson Mass**

Christopher P. Hays

*University of Oxford, Oxford OX1 3RH, United Kingdom*

(for the CDF Collaboration)

Abstract

The first measurement of the  $W$  boson mass ( $m_W$ ) in Run II of the Tevatron Collider has been made by the CDF Collaboration, and is the single most precise  $m_W$  measurement to date. The measurement of  $m_W = 80.413 \pm 0.048$  GeV has a relative precision of 0.06% and results in a new world-average  $m_W$  of  $80.398 \pm 0.025$  GeV. The precise knowledge of  $m_W$  constrains the properties of new hypothetical particles coupling to electroweak gauge bosons.

## 1 Introduction

The unification of the electromagnetic and weak forces includes mixing between the fundamental  $SU(2)$  and  $U(1)$  symmetries. This mixing is parametrized by  $\sin^2 \theta_W \equiv 1 - m_W^2/m_Z^2$ , where  $m_W$  and  $m_Z$  are the masses of the  $W$  and  $Z$  gauge bosons that transmit the weak force. Precise measurements of electroweak parameters provide stringent tests of the theory and constrain the existence of new hypothesized particles coupling to the  $W$  and  $Z$  bosons. The measurement of  $m_W$  is an example of such a test.

In the electroweak theory,  $m_W$  is predicted to be <sup>1)</sup>:

$$m_W^2 = \frac{\pi \alpha_{EM}}{\sqrt{2} G_F \sin^2 \theta_W (1 - \Delta r)}, \quad (1)$$

where  $\alpha_{EM}$  is the electromagnetic coupling at the renormalization scale  $Q = m_Z$ ,  $G_F$  is the Fermi weak coupling extracted from the muon lifetime, and  $\Delta r$  includes all radiative corrections.<sup>1</sup> Since the input parameters have been measured to high precision (better than a part in 10,000), the  $m_W$  measurement is sensitive to loop corrections from particles with weak couplings. For example, the existence of the unobserved Higgs boson would reduce  $m_W$  by a value proportional to the logarithm of the Higgs mass ( $m_H$ ). For a relative  $m_W$  accuracy of 0.03%,  $m_H$  is constrained by  $m_W$  to within  $\approx 50\%$  <sup>2)</sup>.

Previous  $m_W$  measurements at the Large Electron Positron (LEP) and Tevatron colliders have a combined relative  $m_W$  precision of 0.036% <sup>1)</sup>. The first  $m_W$  measurement at Run II of the Tevatron collider has been performed by the CDF Collaboration, and is the single most precise  $m_W$  measurement to date. Incorporating the new CDF measurement into the world-average  $m_W$  fit results in a relative  $m_W$  accuracy of 0.031% <sup>3)</sup>.

## 2 CDF II Detector and Model

The Run II CDF detector <sup>3)</sup> (CDF II) measures particles resulting from  $\sqrt{s} = 1.96$  Tev  $p\bar{p}$  collisions. The detector consists of concentric cylindrical layers surrounding the beam line, each with a particular focus: the inner silicon tracker measures charged-particle trajectories close to the interaction, allowing a precise determination of the interaction point; the outer drift chamber (COT) measures charged-particle momenta transverse to the beam line ( $p_T$ ) with a precision of  $\delta p_T/p_T \approx 0.05\% p_T$ , after a constraint to the interaction region; the 1.4 T solenoid produces a near uniform magnetic field inside the tracking volume; the electromagnetic (EM) calorimeter

---

<sup>1</sup>The convention  $\hbar \equiv c \equiv 1$  is used throughout.

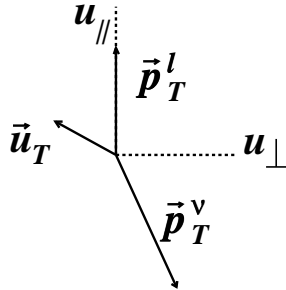


Figure 1: A  $W$  boson event, with the recoil hadron momentum ( $\vec{u}_T$ ) separated into axes parallel ( $u_{\parallel}$ ) and perpendicular ( $u_{\perp}$ ) to the charged lepton.

measures the energy ( $E$ ) of electron and photon showers to a precision of  $\delta E/E \approx \sqrt{0.135^2/E_T + 0.017^2}$ ; the hadronic calorimeter measures hadronic showers to a precision of  $\delta E_T/E_T \approx 80\%/E_T$ ; and the muon drift chambers identify muons penetrating the detector.

The CDF II detector model used in the  $m_W$  measurement consists of a fast parametrized simulation of the components relevant to the measurement. Using a three-dimensional lookup table of the tracking detector's properties, the simulation models ionization energy loss, multiple Coulomb scattering, electron bremsstrahlung, photon conversion, and photon Compton scattering in the tracker. Electron energy loss in the solenoid (before entering the EM calorimeter) and in the hadronic calorimeter (after passing through the EM calorimeter) are parametrized from a GEANT-based detector simulation. Lepton and recoil reconstruction and selection are also modelled in the simulation, whose final products are templates of the distributions used to fit the data.

### 3 CDF $m_W$ Measurement

To date, the Tevatron collider has produced more than  $2.5 \text{ fb}^{-1}$  of  $\sqrt{s} = 1.96 \text{ TeV}$   $p\bar{p}$  collision data per experiment. The first  $m_W$  measurement<sup>3)</sup> is based on  $\approx 200 \text{ pb}^{-1}$  of CDF data, which contain 51,128 (63,964) resonantly produced  $W$  bosons decaying to muons (electrons) after event selection. The selection requires  $30 \text{ GeV} < p_T^l < 55 \text{ GeV}$ ,  $30 \text{ GeV} < p_T^\nu < 55 \text{ GeV}$ ,  $60 \text{ GeV} < m_T(l, \nu) < 100 \text{ GeV}$ , and recoil  $u_T < 15 \text{ GeV}$  (Fig. 1), where

$$m_T = \sqrt{2p_T^l p_T^\nu [1 - \cos \Delta\phi(l, \nu)]}. \quad (2)$$

A sample of 4,960 (2,919) resonantly produced  $Z$  bosons decaying to muons (electrons) provides an important control and is used to fit for the

lepton momentum scale and the recoil model parameters.

### 3.1 Strategy

The  $m_W$  measurement relies on a precise calibration of the lepton momenta in the event. Muon momenta are measured with the tracker, which is calibrated using the muonic decays of the  $J/\psi$  and  $\Upsilon$  quarkonia states, and of the  $Z$  boson. Electron momenta are measured with the calorimeter, which is calibrated using the ratio of calorimeter energy to track momentum ( $E/p$ ) in  $W$  boson events, and using  $Z \rightarrow ee$  events. Neutrino momenta are inferred from the energy imbalance in the event, and their measurement relies on charged lepton and recoil momenta calibrations.

The recoil momentum in a  $W$  or  $Z$  boson event is measured as the net momentum in the calorimeter, excluding the contribution(s) from the charged lepton(s). The measurement includes the underlying event and additional  $p\bar{p}$  interactions, which reduce the resolution of the recoil measurement. The recoil is modelled using a parametrization of the components, with parameters fit using  $Z$  boson data.

The measurement was performed blind, with a single offset applied to the final  $m_W$  fits to the measurement distributions ( $m_T$ ,  $p_T^l$ , and  $p_T^{\nu}$ ). The offset was drawn from a flat distribution between -100 MeV and 100 MeV, and was not removed until the full analysis was complete.

### 3.2 Track Momentum Calibration

Non-uniformities in the tracker are studied with cosmic ray muons, and alignment corrections are applied when fitting the track parameters. The corrections adjust the positions of each 12-wire cell at each end of the COT, and the shapes of the wires within the tracker. Biases in the measured track curvature are studied by comparing the  $E/p$  distributions of electrons and positrons. Differences in  $E/p$  as functions of polar ( $\theta$ ) and azimuthal ( $\phi$ ) angle are removed by correcting the measured track curvature (Fig. 2). The statistical uncertainties on the corrections result in a 6 MeV uncertainty on the  $m_W$  measurement.

Using 606,701  $J/\psi \rightarrow \mu\mu$  candidates, the dimuon invariant mass distribution around  $m_{\mu\mu} = 3.08$  GeV is fit for  $m_{J/\psi}$  as a function of the mean inverse momentum  $\langle p_T^{-1} \rangle$  of the two muons. By comparing the fit result to the world-average  $m_{J/\psi}$  value <sup>1)</sup>, a momentum scale correction  $\Delta p/p$  is derived (Fig. 3). To obtain zero slope in  $\Delta p/p$  as a function of  $\langle p_T^{-1} \rangle$ , a correction is applied to the simulated energy loss in the silicon tracker, effectively reducing the amount of material by 6% relative to the CDF standard value. The dominant uncertainty of  $\sigma_{\Delta p/p} = 0.02\%$  on this calibration arises from the energy loss model.

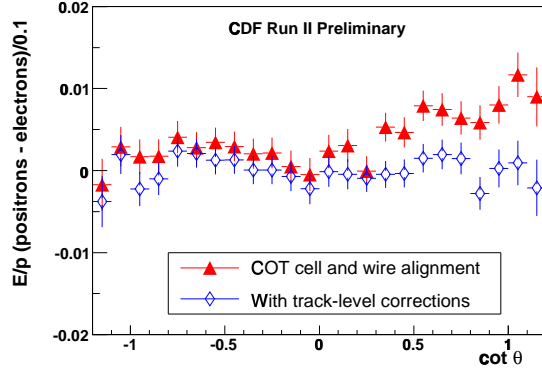


Figure 2: *The difference in  $E/p$  between electrons and positrons, as a function of  $\cot \theta$ , before and after curvature corrections are applied to the reconstructed track.*

An additional track momentum calibration results from fits for  $m_\Upsilon$  to the dimuon invariant mass distribution around  $m_{\mu\mu} = 9.43$  GeV. The measurement is performed both using tracks constrained to the interaction and unconstrained tracks. Comparisons of the two fit results verify that there is no significant bias ( $\sigma_{\Delta p/p} = 0.006\%$ ) from the constraint. The  $\Delta p/p$  extracted from the  $\Upsilon$  measurement is consistent with that obtained from the  $J/\psi$  measurement (Fig. 3), and the two results are combined to give an accuracy of  $\sigma_{\Delta p/p} = 0.019\%$ .

Given this track momentum calibration, the  $Z$  boson mass is measured using its decay to muons. Fitting the dimuon mass distribution for  $m_Z$  around  $m_{\mu\mu} = 91.19$  GeV, a value of  $(91.184 \pm 0.043_{stat})$  GeV is obtained (Fig. 4), consistent with the world average value<sup>1)</sup>. This measurement is incorporated into the calibration, but does not significantly reduce its uncertainty. The combined track calibration and alignment uncertainty corresponds to an uncertainty of  $\delta m_W = 17$  MeV.

### 3.3 Electron Energy Calibration

The calorimeter energy is calibrated using the  $E/p$  distribution of electrons from  $W \rightarrow e\nu$  decays, and the dielectron mass distribution from  $Z \rightarrow ee$  decays. The  $E/p$  calibration relies on an accurate modelling of the electron energy loss in the tracker, which is tested by measuring  $m_Z$  with the dielectron invariant mass using the track momentum measurement. The result is consistent with the world average value<sup>1)</sup>, within the 143 MeV uncertainty of the measurement. An additional validation of the simulation is the modelling of the data  $E/p$  distribution (Fig. 5). Electron shower leakage into the hadronic calorimeter

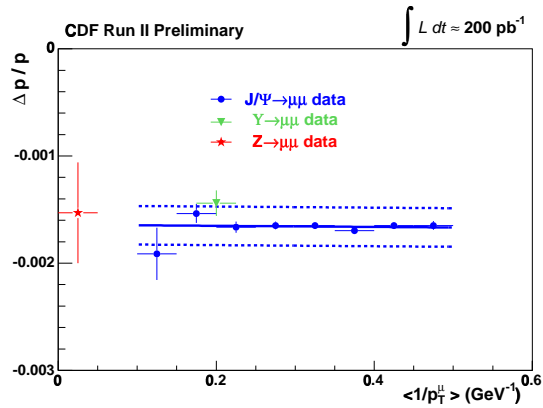


Figure 3: The track momentum scale correction obtained from fits to the dimuon mass distribution for  $J/\psi$ ,  $\Upsilon$ , and  $Z$  boson decays to muons. The dashed line is the systematic uncertainty on the  $J/\psi$  measurements, and the error bars indicate statistical uncertainties.

and energy loss in the tracker are the dominant effects in the regions above and below the  $E/p$  peak, respectively. The region above the peak is used to fit for an energy loss scale in the tracker simulation, and the result is consistent with a scale of 1. This result is different than for muons because muons have a different dependence on material type, and the mixture of material types in the standard CDF simulation may be inaccurate at the few percent level. The relative statistical uncertainty on the  $E/p$  calibration is 0.034%.

The calorimeter energy scale can have an energy dependence due to variations in response as a function of shower depth, or mismodelling of shower leakage into the hadronic calorimeter or energy loss in the tracker. This energy dependence, or “non-linearity,” is measured by fitting the  $E/p$  peak as a function of  $E_T$  in  $W$  and  $Z$  boson events. A non-linear effect with a statistical significance of  $1\sigma$  is applied as a correction to the simulation. The uncertainty on the non-linearity measurement corresponds to a 23 MeV uncertainty on  $m_W$ .

As a test of the  $E/p$  calibration, and to improve the accuracy of the calorimeter energy calibration, the dielectron mass distribution around  $m_{ee} = 91.19$  is fit for  $m_Z$  (Fig. 6). The fit result is consistent with the world average value of  $m_Z$ , which is used as an additional calibration constraint. The total uncertainty of the calorimeter energy scale corresponds to an uncertainty  $\delta m_W = 30$  MeV in the electron channel.

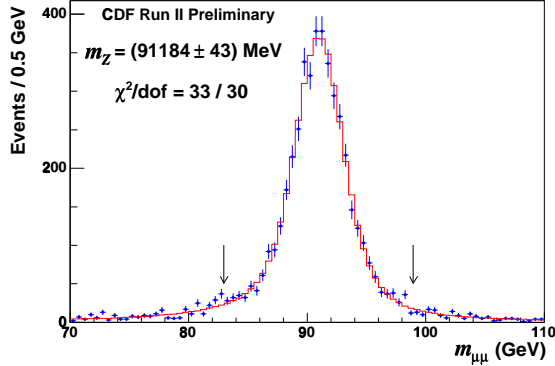


Figure 4: *The fit for  $m_Z$  to the dimuon mass distribution. The arrows indicate the fit region and the uncertainty is statistical only.*

### 3.4 Recoil Calibration

The recoil momentum scale is modelled as a logarithmic function of recoil momentum. The two fit parameters in the function determine the scale at zero momentum and the rate of scale increase with increasing momentum. The parameters are determined from fits to the balance between recoil and lepton momenta in  $Z$  boson events.

The recoil momentum resolution is assumed to arise from stochastic fluctuations in the calorimeter, taking the form  $\sigma_{u_T} \propto \sqrt{u_T}$ . Additional resolution from the underlying event and additional  $p\bar{p}$  interactions is modelled by adding energy in the simulation using a distribution derived from generic interaction data. The additional energy includes a scale parameter to allow for a difference between underlying event energy in generic interactions and in  $Z$  boson data. Both the proportionality constant in the recoil resolution function and the scale parameter for the underlying event are determined from a fit to the rms of the momentum balance between the recoil and leptons in  $Z$  boson events.

The recoil model is tested with distributions from  $W$  boson events. A particularly relevant distribution is the recoil parallel to the charged lepton ( $u_{||}$ ), since to first order  $m_T$  can be approximated by  $2p_T^l + u_{||}$  (using  $p_T^l \approx |p_T^l + u_{||}|$ ). The simulation accurately predicts the mean and rms of this distribution (Fig. 7).

### 3.5 Production Model and Backgrounds

$W$  and  $Z$  boson events are simulated using the RESBOS event generator<sup>4)</sup>, with the CTEQ6M input parton distribution functions<sup>5)</sup>. The generator pro-

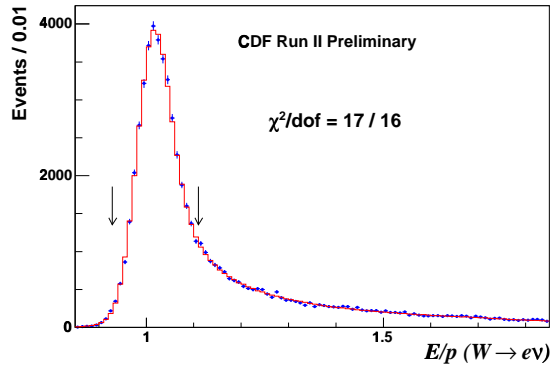


Figure 5: *The fit for the calorimeter energy scale to the peak of the  $E/p$  distribution. The arrows indicate the fit region.*

vides a next-to-leading-log resummation of the QCD corrections, as well as a parametrization of the non-perturbative regime. CDF constrains the parameters using the  $Z$  boson  $p_T$  distribution, and the resulting uncertainty on the  $m_T$  fit for  $m_W$  is 3 MeV. The uncertainty on the model of parton distribution functions is determined using the 90% confidence level (CL) eigenvector uncertainties, and the corresponding  $1\sigma$  uncertainty is  $\delta m_W = 11$  MeV for the  $m_T$  fit.

Photon radiation from the final-state charged lepton is modelled with energy and angular distributions extracted from a next-to-leading-order event generator (WGRAD) <sup>6)</sup>. Higher-order corrections are implemented by scaling up the extracted photon energy by 10%, and a 5% uncertainty is applied. The total uncertainty from photon radiation is  $\delta m_W = 8(9)$  MeV for the electron (muon)  $m_T$  fit.

Backgrounds to the  $W$  boson event sample consist of electroweak boson decays, modelled with the standard CDF simulation, and hadrons and cosmic rays, modelled with the data. The hadronic background can result from jet production, with a high-momentum hadron decaying leptonically, or from a kaon or pion decay in flight, with the decay muon momentum mismeasured. The largest background of 6.6% results from  $Z \rightarrow \mu\mu$  events, where one of the muons is outside the fiducial volume ( $|\eta| < 1$ ) of the COT. Uncertainties on the background prediction result in uncertainties of  $\delta m_W = 11(12)$  MeV for the electron (muon)  $m_T$  fit.

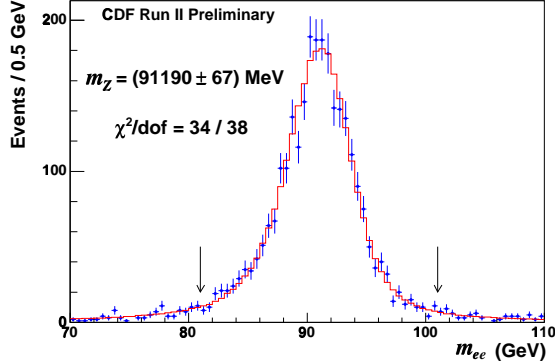


Figure 6: *The fit for  $m_Z$  to the dielectron mass distribution. The arrows indicate the fit region and the uncertainty is statistical only.*

Table 1: *Backgrounds to the  $W$  boson event sample.*

Background	$W \rightarrow \mu\nu$ (%)	$W \rightarrow e\nu$ (%)
$Z \rightarrow ll$	$6.6 \pm 0.3$	$0.24 \pm 0.04$
$W \rightarrow \tau\nu$	$0.89 \pm 0.02$	$0.93 \pm 0.03$
Hadronic jets	$0.1 \pm 0.1$	$0.25 \pm 0.15$
Decays in flight	$0.3 \pm 0.2$	-
Cosmic ray muons	$0.05 \pm 0.05$	-

### 3.6 Mass Fits and Results

The  $W$  boson mass is fit using the  $m_T$  (Fig. 8),  $p_T^l$ , and  $p_T^{\bar{l}}$  distributions (Table 2). The  $m_T$  fit has an 80% weight in the combination of the results, which is  $m_W = 80.413 \pm 0.048$  GeV.

## 4 Summary and Outlook

The CDF Collaboration has made the most precise single  $m_W$  measurement to date. The new world average of  $m_W = 80.398 \pm 0.025$  GeV has a relative uncertainty of 0.031%. Combining the  $m_W$  measurement with measurements of other electroweak parameters <sup>1)</sup>, the Higgs mass is predicted to be  $m_H = 76_{-24}^{33}$  GeV, or  $m_H < 144$  GeV at 95% CL <sup>3)</sup>. With a factor of  $\approx 10$  increase in data already collected, CDF expects its next measurement to have a precision better than 25 MeV.

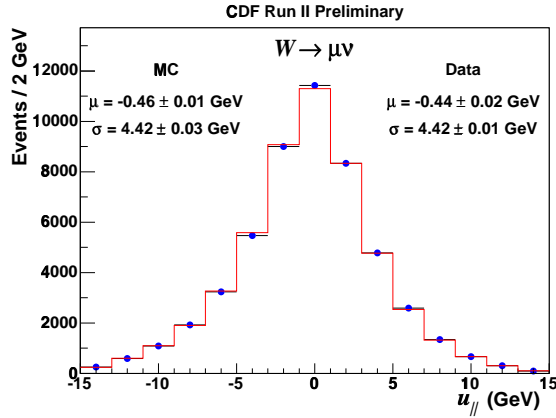


Figure 7: The data (circles) and simulation (histogram)  $u_{||}$  distributions for  $W \rightarrow \mu\nu$  data. The uncertainties on the data are statistical, and the uncertainties on the simulation result from uncertainties on the recoil model parameters derived from  $Z \rightarrow ee$  and  $Z \rightarrow \mu\mu$  data.

Table 2: The results of the fits for  $m_W$  to the  $m_T$ ,  $p_T^l$ , and  $p_T^\nu$  distributions in the electron and muon decay channels.

Distribution	$m_W$ (GeV)	$\chi^2/\text{dof}$
$m_T(e, \nu)$	$80.493 \pm 0.048_{stat} \pm 0.039_{sys}$	86/48
$p_T^l(e)$	$80.451 \pm 0.058_{stat} \pm 0.045_{sys}$	63/62
$p_T^\nu(e)$	$80.473 \pm 0.057_{stat} \pm 0.054_{sys}$	63/62
$m_T(\mu, \nu)$	$80.349 \pm 0.054_{stat} \pm 0.027_{sys}$	59/48
$p_T^l(\mu)$	$80.321 \pm 0.066_{stat} \pm 0.040_{sys}$	72/62
$p_T^\nu(\mu)$	$80.396 \pm 0.066_{stat} \pm 0.046_{sys}$	44/62

## References

1. W.-M. Yao *et al.*, J. Phys. G **33**, 1 (2006).
2. M. Awramik *et al.*, Phys. Rev. D **69**, 053006 (2004).
3. CDF Collaboration, to be submitted to Phys. Rev. D.
4. F. Landry, R. Brock, P. M. Nadolsky, and C.-P. Yuan, Phys. Rev. D **67**, 073016 (2003).
5. J. Pumplin *et al.*, Jour. High En. Phys. 0207, 012 (2002).
6. U. Baur, S. Keller and D. Wackerroth, Phys. Rev. D **59**, 013002 (1998).

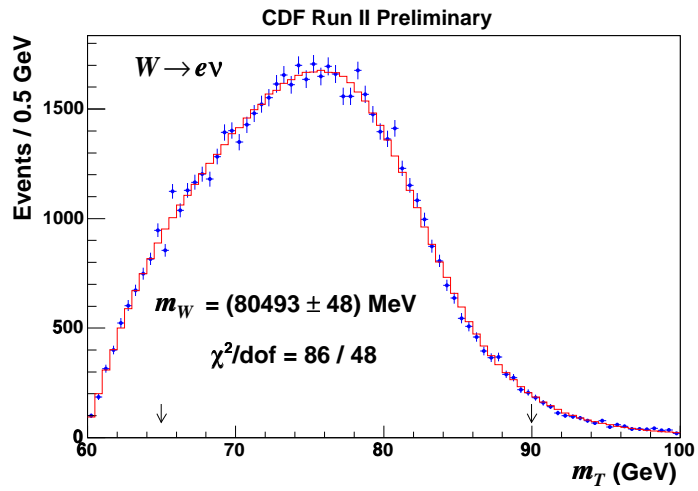
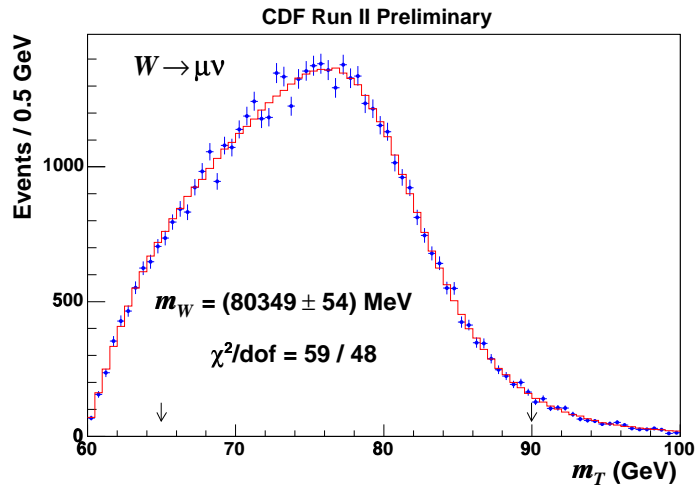


Figure 8: The fits for  $m_W$  to the  $m_T$  distribution in  $W \rightarrow \mu\nu$  (top) and  $W \rightarrow e\nu$  (bottom) events. The arrows indicate the fit regions and the uncertainties are statistical only.